has been incorporated into a production oriented three-dimensional finite element code called NEPSAP. Applications of the code for the collapse analysis of a number of classical and production-type problems with composite construction were illustrated.

References

[1] Sharifi, P. and Yates, D. N., "Nonlinear Thermo-Elastic-Plastic and Creep Analysis by the Finite Element Method," *AIAA Journal*, Vol. 12, Sept. 1974, pp. 1210–1215.

[2] Clough, R. W. and Felippa, C. A., "A Refined Quadrilateral Element for Analysis of Plate Bending," *Proceedings of Second Conference on Matrix Methods in Structural Mechanics*, AFFDL-TR-68-150, Oct. 1968, Air Force Flight Dynamics Lab., Wright-Patterson Air Force Base, Ohio, pp. 399–440.

[3] Suarez, J. A., "Advanced Composite Wing Structures, Stability Analysis of Advanced Filamentary Composite Panels," Tech. Rept. AC-SM-8087, May 1970, Grumman Aircraft Engineering Corp., Bethpage, N.Y.

[4] Kaminski, B. E. and Ashton, J. E., "Diagonal Tension Behavior of Boron-Epoxy Shear Panels," *Journal of Composite Materials*, Vol. 5, Oct. 1971, pp. 553–558.

[5] Bushnell, D., "Stress, Stability, and Vibration of Complex Branched Shells of Revolution: Analysis and User's Manual for BOSOR4," LMSC-D243605, March 1972, Lockheed Missiles & Space Co., Sunnyvale, Calif. Also CR 2116, Oct. 1972, NASA.

JUNE 1975 AIAA JOURNAL VOL. 13, NO. 6

Fracture Mechanics Application of an Assumed Displacement Hybrid Finite Element Procedure

SATYA N. ATLURI*
Georgia Institute of Technology, Atlanta, Ga.
AND
ALBERT S. KOBAYASHI† AND MICHIHIKO NAKAGAKI‡
University of Washington, Seattle, Wash.

An assumed displacement hybrid finite element procedure developed specifically for treating mixed-mode behavior of cracks was used to solve two-dimensional problems in fracture mechanics involving anisotropic, nonhomogeneous but linearly elastic materials. The procedure was then checked by analyzing problems with known solutions which include centrally cracked isotropic and orthotropic tension plates, single-edge-notched tension plate, oblique edge-notched tension plate, and tension plates with one-quarter circular crack and subjected to uniaxial or biaxial tension. Also a doubly edge-cracked orthotropic tension plate and an orthotropic three point bend specimen, for which theoretical solutions are not available, were analyzed.

I. Introduction

DURING the past decade fracture mechanics has been successfully used to analyze failed parts,[1,2] certifying a structure for its intended use,[3] and correlating cyclic or sustained stress crack growth[4] of flaws. In applying fracture mechanics to practical problems, however, the analyst must know the stress intensity factor of a flawed structure as well as the stress intensity factors of laboratory specimens used to establish material characteristics such as the fracture toughness, cyclic crack growth rates, and sustained stress crack growth rates. Unfortunately, available solutions of stress intensity factors are limited to idealized flaws of simple geometries and loading conditions and thus require considerable engineering judgment before they can be used to estimate stress intensity factors of complex flaws which exist in actual problems. It is also short of impossible to solve these practical problems by the elegant but laborious analytical procedures used by others.[5]

For two-dimensional problems in fracture mechanics, the method of finite element analysis which is a well-developed and widely used numerical technique in structural analysis[6] can be used to determine the stress intensity factor for a single mode,[7–12] as well as mixed mode of crack-tip deformation. For such elastic analysis, the stress singularity at the crack tip requires that small elements be used in the vicinity of the crack tip if the near-field stresses are to be accurately calculated. To circumvent such refinement, crack opening displacements[7,8] and more recently the strain energy release rate[9,10] have been used to estimate stress intensity factors with relatively coarse finite element grids. Although the crack opening displacement (COD) approach enables one to determine the opening mode and sliding mode stress intensity factors, the numerical accuracy of this approach leaves much to be desired. On the other hand, the approach by elastic strain energy release rate provides better accuracy but the two modes of crack-tip deformation cannot be separated.

Other approaches in determining the stress intensity factors by the method of finite element analysis involve developing super elements with various embedded stress singularity.

Presented as Paper 74-390 at the AIAA/ASME/SAE 15th Structures, Structural Dynamics and Materials Conference, Las Vegas, Nevada, April 17–19, 1974; submitted April 12, 1974; revision received November 22, 1974. The authors wish to express their gratitude to W. J. Walker, Air Force Office of Scientific Research, for his continuous support and encouragement. This work was supported by the Air Force Office of Scientific Research under Grant AFOSR-73-2478.

Index category: Structural Static Analysis.

* Associate Professor, School of Engineering Science and Mechanics.

† Professor, Department of Mechanical Engineering.

‡ Graduate Student, Department of Mechanical Engineering. Presently, Post Doctoral Fellow at Georgia Institute of Technology.

Byskov[11] and Tracey[12] used elements with displacement fields which were incompatible with those of the adjacent elements. In each case, the accuracy of stress intensity factor determination increased. Pian et al.[13] improved substantially the efficiency of this method by using a hybrid stress model[14] which incorporates the stress intensity factor as an unknown in the final matrix equation. As a result, they practically eliminated the requirements of refined elemental breakdown for solving a class of fracture problems by the method of finite element analysis. The purpose of this paper is to present another approach, namely the hybrid displacement model, which has been used successfully by Tong[15] in plate problems and Atluri[16] in shell bending problems, in solving two-dimensional problems in fracture mechanics.

II. Theoretical Background

The theoretical basis of the assumed displacement hybrid model[15,16] is a modified principle of minimum potential energy for which the functional to be varied is

$$\pi_{H_D}(u_i, v_i, T_{L_i}) = \sum_m \left\{ \int_{V_m} (\tfrac{1}{2} E_{ijkl}\, \varepsilon_{ij}\, \varepsilon_{kl} - \overline{F}_i\, u_i)\, dv + \int_{\partial V_m} T_{Li}(v_i - u_i)\, ds - \int_{S_{\sigma_m}} \overline{T}_i\, v_i\, ds \right\} \quad (1)$$

where V_m is the volume of mth element, ∂V_m is the boundary of V_m, S_{σ_m} is the portion of ∂V_m where surface tractions $\overline{T}_i$ are given, and E_{ijkl} are the given elastic constants. In Eq. (1)

$$\varepsilon_{ij} = \tfrac{1}{2}(u_{i,j} + u_{j,i})$$

where u_i are differentiable displacements within V_m, but need not be continuous across the boundary of V_m. The functions, v_i, are the inter-element boundary displacements which are continuous on ∂V_m and subject to the condition of $v_i = u_i$ on S_{u_m}, where S_{u_m} is the portion of ∂V_m over which displacements u_i are assigned. $\overline{F}_i$ is the body force and T_{Li} is the boundary traction on ∂V_m. As has been shown in Ref. 17, the variational equation $\delta\pi_{HD} = 0$ with respect to admissible variational δu_i, δT_{Li} and δv_i, leads to the following Euler equations where: 1) Displacements u_i in V_m generate stresses of $\frac{1}{2}E_{ijkl}(u_{k,l} + u_{l,k})$ which satisfy local equilibrium in V_m. 2) u_i at ∂V_m coincide with interelement boundary displacement, v_i, which is independently assumed. Since v_i is the same for two adjacent elements on their common boundary, this equation thus enforces, a posteriori, the condition that u_i of one element is equal to u_i of its neighboring element at their common boundary. 3) The boundary tractions, T_{Li}, which are treated as independent unknowns in the present problem coincide with the tractions $\frac{1}{2}E_{ijkl}(u_{k,l} + u_{l,k})v_j$ generated at ∂V_m by u_i.

Thus in constructing the finite element model one assumes: a) displacement field in the interior of each element that need not satisfy any criteria of compatibility at the interelement boundary; b) an independent displacement field at the boundary of each element that is inherently compatible with the boundary displacement of neighboring elements; and c) an independent set of boundary tractions. Other theoretical details of the formulation are given in Ref. 17.

Briefly, the finite element program based on this procedure, for arbitrary loading and boundary conditions, uses four "singular" elements which surround the crack tip and "regular" elements which occupy the remaining region. The regular element incorporates an inherently compatible, quadratic boundary and quadratic interior displacement field and a quadratic set of Lagrange multiplier boundary tractions. The singular element incorporates a displacement field of $(r)^{1/2}$ type with the two modes of stress intensity factors, K_I and K_{II} as unknowns, as well as boundary displacements and Lagrangian multiplier boundary tractions with the correct built-in singular behavior. Displacement compatibility between such "singular" elements and "regular" elements is also maintained. Isoparametric transformations are used to derive the stiffness matrix of quadrilateral elements whose boundaries are curved and thus the developed

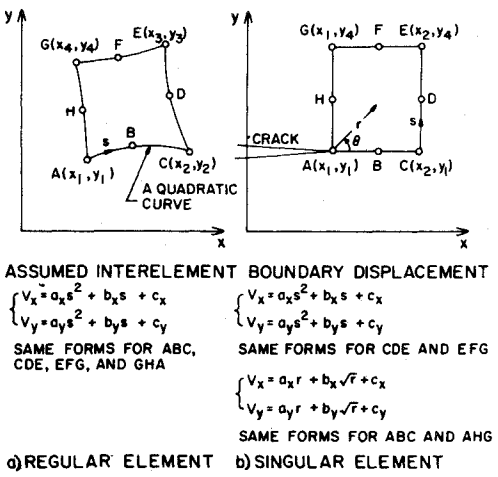

Fig. 1 Finite elements and interelement boundary displacements.

procedure is also suitable for analyzing the mixed-mode behavior of curved cracks in a plate composed of anisotropic, nonhomogeneous, but linearly elastic material. In the following, computational details which are important for successful computer runs but which do not add materially to the theoretical background are described.

A. Boundary Displacement for the Singular Element

As described in Ref. 17, the interelement boundary displacements of the regular elements were assumed to be a quadratic polynomial of an $as^2 + bs + c$ where s is the distance measured along the generally curved element boundary shown in Fig. 1a. a, b, and c are unique coefficients determined by the nodal displacements at the 3 nodes, say A, B, and C, in Fig. 1a. The latter assures interelement displacement compatibility since these nodes are common for elements that share the common boundary.

For the singular elements, however, the boundary displacements were assumed to be $ar + b(r)^{1/2} + c$ where r is the radial distance from the crack tip as shown in Fig. 1b. The choice of this displacement function was obviously influenced by the known elastic distribution of the displacement near the crack tip.[18] This displacement distribution, when used along the two interelement boundaries not sharing the crack tip, such as CDE and EFG in Fig. 1b, resulted in as much as 15% discrepancies between the fitted and the correct displacement distributions in the vicinity of the crack tip. These differences are illustrated in Fig. 2. Hindsight dictates that while the fitted displacements should agree exactly with the correct displacement distribution, such agreement could not generally be expected in a fitted displacement distribution which cannot vary with the angular orientation of θ. In fact the quadratic displacement function of $as^2 + bs + c$ was found to fit better with the correct displacements along the two sides of CDE and EFG of the singular element in Fig. 1b, and thus this displacement function was used for these two sides.

B. Boundary Traction for the Singular Element

The boundary traction T_{Li} in this assumed displacement hybrid finite element method is mathematically a Lagrangian multiplier. As such one can assume any convenient form for T_{Li}. For better numerical accuracy, however, the assumed T_{Li} should match the traction force derived from the distribution of interior displacement u_i of the element of

$$T_{Li} = \tfrac{1}{2}E_{ijkl}(u_{k,l} + u_{l,k}) \cdot v_j \quad (2)$$

where E_{ijkl} is elastic-compliance tensor and v_j is the direction of cosines of the surface normal to the boundary. Since the assumed interior displacement for the singular element contains an $(r)^{1/2}$ distribution, the right-hand side of Eq. (2) will contain a $1/(r)^{1/2}$

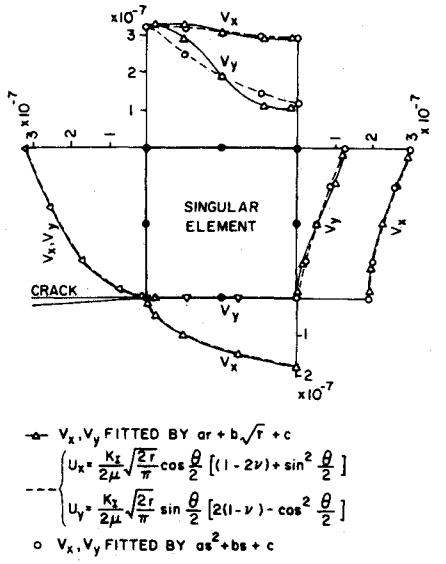

Fig. 2 Alternate interelement boundary displacements on singular element.

singularity. Thus for accurate matching of the left and right-hand sides of Eq. (2), this $1/(r)^{1/2}$ singularity must be incorporated into the assumed boundary traction T_{Li}. Numerical experimentation verified that indeed the stress intensity factor can be more accurately determined when the surface traction, T_{Li}, for this singular element contains the correct singularity of $1/(r)^{1/2}$.

To incorporate the proper singularity terms into these boundary tractions for arbitrary-shaped elements with curved boundaries, first some stress functions were assumed in the interior of the element. These stress functions contained the proper singular terms, and satisfied the homogeneous equilibrium equations. The assumptions for Lagrangian multiplier boundary tractions, necessary in this formulation, were then assumed to correspond with the boundary traction field generated by the stresses derived from the previous stress functions. It has also been demonstrated in the present work that by properly assuming the singular boundary traction field in the singular elements and satisfying the stress-free conditions, the numerical accuracy of the stress-intensity factor determination increased by 20–30%.

Since the boundary tractions T_{Li} are assumed independently in this assumed displacement hybrid finite element approach, the stress-free boundary conditions on the crack surface can be easily imposed on the appropriate singular as well as regular elements which adjoin the crack surface. This is in contrast to the assumed stress hybrid model (in which equilibrating stresses in the interior and compatible displacements on the boundary of the element are assumed), wherein the coefficients of the stress field in the interior of the element must be so constrained, a priori, such that they result in zero tractions at the boundary.§ Such a procedure is, in general, very difficult to impose on elements with arbitrary shaped boundaries.

C. Singular Stress Field

As shown by Eq. (1), an area integral involving the strain energy density must be evaluated in order to construct the element "stiffness" equations. For a "singular" element, wherein the assumed displacement field involves a combination of regular polynomial type and $(r)^{1/2}$ type of behavior, it can be seen that this strain energy density involves tensor inner products of the following three types: a) product of the regular polynomial tensors; b) product of singular tensors of $1/(r)^{1/2}$ type; and c) product of regular and singular tensors. Evaluation of area integrals involving types a and c of these integrals is carried out in the present computer program by transforming them to line integrals along the element boundaries by using the divergence theorem following Ref. 13. The known distribution of singular stress tensor, which is equilibrated, was used to eliminate the direct numerical determination of such stresses from the assumed $(r)^{1/2}$ type displacement fields. Numerical experimentation showed that this indirect procedure of using known distribution of singular stresses yielded results identical within at least 5–6 digits of the indirect procedure but saved some computational time.

Also wherever numerical integration of terms involving $1/(r)^{1/2}$ was involved, these terms were transformed by t where $r = t^2$ thus reducing the line integration along the transformed element to ordinary Gaussian integration with limits from -1 to $+1$.

D. Optimum Size of Singular Element

The question regarding convergence of the finite element solution for smaller singular elements was discussed qualitatively in Ref. 17. In this paper, it was concluded that an optimum singular element size existed for the finite element procedure which intermixed regular and singular elements used in this investigation. The validity of such conclusion was indicated in some preliminary results involving a centrally cracked tension plate.[17] This particular numerical experimentation was carried out further and these results are described in the following.

The test case involved the well-analyzed centrally cracked tension plate[20] shown in the legend of Fig. 3. The nominal value of stress intensity for this problem is $K_I = 3.058$. A quadrant of this tension plate with different sizes of singular element but with fixed number of 24 elements; i.e., 22 regular elements and 2 singular elements, was analyzed. The singular elements were square in all computations. Since the accuracy of stress intensity factor determination is governed by both the sizes of singular and regular elements, attempts were made to systematize the variations in regular elements such that these variations would not impose undue irregular fluctuations in the stress intensity factors. The 4 and 6 regular elements sharing the same row and column respectively with the 2 singular elements, obviously, had to be changed together with the change in size of the 2 singular elements. The remaining regular elements in 1 set of numerical experimentations were left unchanged except for the obvious adjustment in the regular elements adjoining the row and 2 columns of regular elements previously described. In another set of numerical experimentation, the relative sizes of the remaining regular elements were maintained; the singular

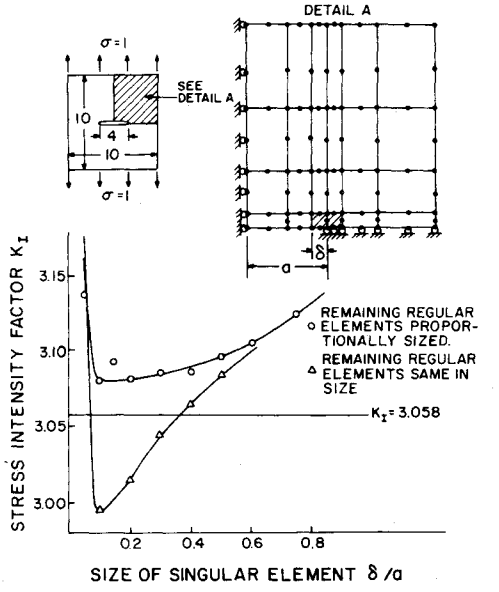

Fig. 3 Variation in stress intensity factor with size in singular element.

§ Atluri has recently shown a convenient procedure for handling the stress-free boundary condition in the assumed stress model.[19]

elements varied in size. Figure 3 shows changes in computed stress intensity factors as the size of singular elements is changed. For this particular problem, an optimum size of the singular element is about $\frac{1}{10}$ of the half crack size when the proportional dimensions of the remaining regular elements are maintained. When much of the original dimensions of the remaining regular elements are maintained, the error in stress intensity factor determination oscillated drastically with the optimum size of the singular element being about 0.35 of the half crack length. It should be noted that other sources of numerical errors, such as the well known numerical instability due to use of oblong quadrilateral elements, could not be eliminated in searching for an optimum size of singular element. The results, thus obtained are valid only for the particular problem and particular element breakdown shown in Fig. 3. Optimum sizes for singular element will vary with the problem and can only be estimated through some form of numerical experimentation at this time.

This example illustrates the sensitivity of this numerical analysis to the choice of the sizes of singular and regular elements. It also shows that the prudent rule of thumb of $\frac{1}{10}$ the half crack length for singular element size established through experience, will in general yield reasonable results in stress intensity factors provided the regular elements are also appropriately spaced.

III. Results

The finite element procedure based on the assumed displacement hybrid model was checked out by analyzing problems with known solutions which include centrally cracked tension plates with different element breakdowns, single-edge-notched tension plate, oblique edge-notched tension plate, and tension plates with one-quarter circular crack under biaxial or uniaxial tension. These results are tabulated in Table 1 with the percentage error in the computed stress intensity factors K_I and K_{II}. Some of these problems, listed in Table 1, have not hitherto been solved by finite element methods.

Detailed discussions on the results of centrally cracked tension plate, edge-cracked tension plate and quarter-circular crack in a tension plate appeared in Ref. 17 and will not be repeated here. At the risk of being repetitious, however, the authors wish to point out again the large discrepancy in the computed stress intensity factors, particularly in K_{II}, and referenced K_{II} for the one-quarter circular crack in a uniaxially loaded tension plate. The K_{II} value computed for the same plate in biaxial tension agreed well with the referenced theoretical result,[18] indicating possible error in the corresponding theoretical result for the uniaxial tension case in Ref. 18. The correct stress intensity factor was later derived and reported in Ref. 17.

Table 1 Solutions to some two-dimensional problems in fracture mechanics by the assumed displacement hybrid finite element procedure

Cracked plate	Mesh size	Computed K_I	Computed K_{II}	Reference K_I	Reference K_{II}	Computed K_I error percent	Computed K_{II} error percent
Center cracked tension plate $c/b = 1$ $a/b = 0.4$ $b = 5$	2 small singular elements 24 elements total	3.08	0.00273	Bowie & Neal[21] 3.06		+0.653	
Center cracked tension plate with orthotropic properties	2 small singular elements 24 elements total	See Fig. 5		Bowie & Freese[20]			
Center cracked tension plate $c/b = 1$ $a/b = 0.4$ $b = 5$	2 large singular elements 12 elements total	3.13	0.0786	Bowie & Neal[21] 3.06		+2.28	
Single edge notch $c/b = 1$ $a/b = 0.4$ $b = 5$	2 singular elements 24 elements total	5.260	−0.06736	Gross, Srawley & Brown[22] 5.289		−0.567	
Oblique edge notch $h/w = 2$ $a/w = 0.4$ $w = 4$	4 singular elements 42 elements total	2.265	1.085	Bowie[19] $K_I = 2.30$	$K_{II} = 1.10$	−1.52	−1.36
Curved cracked uniform tension plate $c/b = 1$ $b = 4$	4 singular elements 48 elements total	1.231	−0.524	Sih, Paris & Erdogan[18] $K_I = 1.201$ (Infinite Plate Solution)	$K_{II} = -0.497$	(2.49)	(5.37)
Curved crack uniaxial tension plate	4 singular elements 48 elements total	0.812	−0.887	$K_I = 0.987$ (Infinite Plate Solution)	$K_{II} = -0.482$	(−17.7)	(84.3)
				$K_I = 0.811$ (Ref. 17) (Infinite Plate Solution)	$K_{II} = 0.906$	(0.12)	(−2.09)

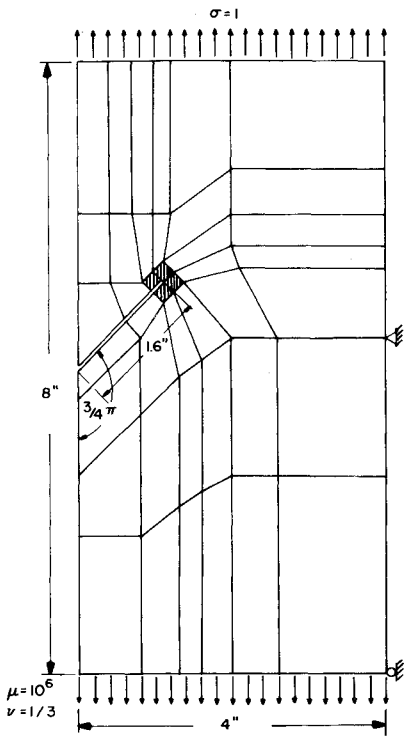

Fig. 4 Element break down for an oblique edged crack in a tension plate.

Figure 4 shows the finite element model, 42 elements and 159 nodes, used for determining mixed-mode stress intensity factors for an oblique edge-notched tension plate. The geometry of the problem precluded further reduction in the number of elements used in this analysis. The 2 stress intensity factors, K_I and K_{II}, were obtained by using this relatively coarse nodal breakdown. The two stress intensity factors, K_I and K_{II}, were within 1.5% of the values reported by Bowie.[21]

The developed procedure was then used to analyze a centrally cracked orthotropic tension plate and compared with the analytical solution by Bowie and Freese.[22] The quadrant composed of 24 elements and 93 nodal breakdowns shown in the legend of Fig. 3 was also used for this study. Principal directions of the orthotropic material were aligned in the 2 lines of symmetry and therefore only 1 quadrant of the plate was considered in this analysis. The material properties being considered are: shear modulus $\mu = 10^6$ psi; Poisson ratio $\nu = \frac{1}{3}$; and ratio of modulus of elasticity, $E_x/E_y = 0.3$, 0.7, 1.0, 1.5, and 4.5. Figure 5 shows the computed variations in stress intensity factors with variations in the ratio of modulus of elasticity. An excellent agreement between the results of finite element analysis and that of Bowie and Freese is noted.

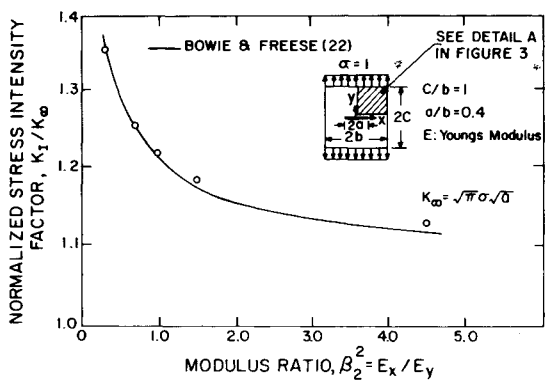

Fig. 5 Stress intensity factor in an orthotropic tension plate with central crack.

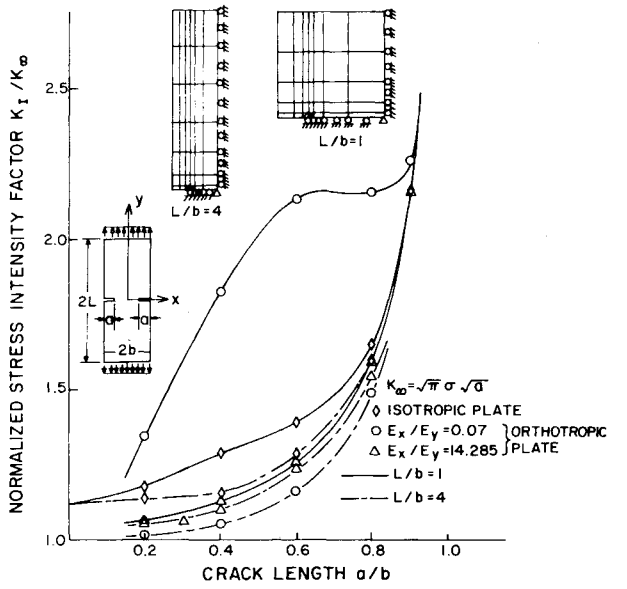

Fig. 6 Stress intensity factor in an orthotropic tension plate with double external cracks.

The legend in Fig. 6 shows element and nodal breakdown of two orthotropic double-edge-cracked tension specimens with aspect ratios of 4 and 1. The material properties were held constant in this case and the crack depth was varied from 0.2–0.8 of half specimen width. Figure 6 shows the variation in stress intensity factor with variation in crack depth for 2 orientations of the principal directions of orthotropic material properties. Noticeable differences in the stress intensity factor with difference in aspect ratios are noted for the material which is very rigid in longitudinal direction. Also noted is the stress intensity factors for shorter crack length which are significantly lower than the theoretical values of 1.12 for isotropic double-edge-notched tension plate with short cracks.

The legend in Fig. 7 shows element and nodal breakdowns of a three-point bend specimen composed of orthotropic materials. Again the material properties were held constant and the stress intensity factors were computed for crack depth from 0.4–0.8 of specimen width for 2 orientations of principal directions of the material properties. Figure 7 also shows a comparison of the computed stress intensity factor and that by Srawley et al.[23] for an isotropic material.

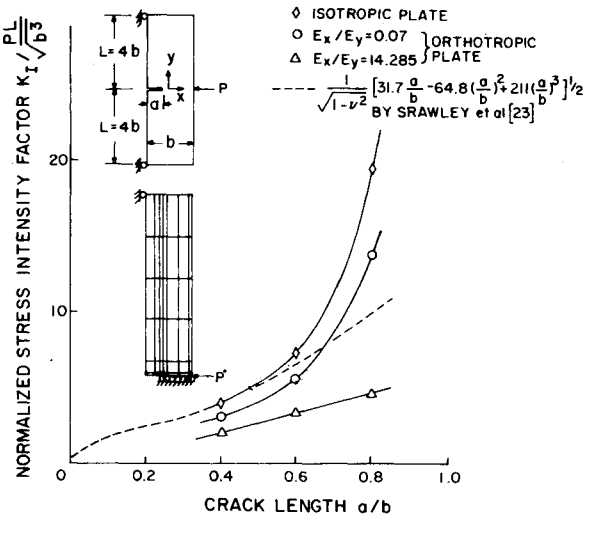

Fig. 7 Stress intensity factor in an orthotropic three point bend specimen.

Conclusion

The utility of the assumed displacement hybrid finite element procedure in determining the stress intensity factor in two-dimensional problems in fracture mechanics has been demonstrated. The existence of an optimum size of singular element was shown by numerical experimentation. Stress intensity factors for orthotropic double-edge-cracked tension specimen and three-point bend specimen were obtained for the first time.

References

[1] Tiffany, C. F. and Masters, J. N., "Applied Fracture Mechanics," ASTM STP 381, June 1964, pp. 249–278.

[2] Srawley, J. E. and Esgar, J. B., "Investigation of Hydrotest Failure of Thiokol Chemical Corporation 260-inch Diameter SL-1 Motor Case," TM X-1194, Jan. 1966, NASA.

[3] Tiffany, C. F., Masters, J. N., and Shah, R. C., "Fracture Control of Metallic Pressure Vessels," SP-8040, 1971, NASA.

[4] Hall, L. R. and Shah, R. C., "On Plane Strain Cycle Flaw Growth Rate," *Engineering Fracture Mechanics*, Vol. 3, July 1971, pp. 169–189.

[5] *Fracture, An Advanced Treatise*, edited by H. Liebowitz, Vols. I and II, Academic Press, New York, 1968.

[6] Zienkiewicz, O. C., *The Finite Element Method in Engineering Sciences*, McGraw-Hill, New York, 1971.

[7] Kobayashi, A. S., Maiden, D. E., Simon, B. J., and Iida, S., "Application of the Method of Finite Element Analysis to Two-Dimensional Problems in Fracture Mechanics," New York, Nov. 1969, ASME Paper 69-WA/PVP-12.

[8] Chan, J. K., Tuba, I. S., and Wilson, W. K., "On the Finite Element Method in Linear Fracture Mechanics," *Engineering Fracture Mechanics*, Vol. 2, July 1970, pp. 1–17.

[9] Watwood, V. B., "The Finite Element Method for Prediction of Crack Behavior," *Nuclear Engineering and Design*, Vol. 11, Sept. 1969, pp. 323–332.

[10] Anderson, G. P., Ruggles, V. L., and Stikor, G. S., "Use of Finite Element Computer Programs in Fracture Mechanics," *International Journal of Fracture Mechanics*, Vol. 7, March 1971, pp. 63–76.

[11] Byskov, E., "The Calculation of Stress Intensity Factors Using the Finite Element Method with Cracked Elements," *International Journal of Fracture Mechanics*, Vol. 6, June 1970, pp. 159–167.

[12] Tracey, D. M., "Finite Elements for Determination of Crack Tip Elastic Stress Intensity Factors," *Engineering Fracture Mechanics*, Vol. 3, July 1971, pp. 255–266.

[13] Pian, T. H. H., Tong, P., and Luk, C. H., "Elastic Crack Analysis by a Finite Element Hybrid Method," presented at 3rd Air Force Conference on Matrix Method in Structural Mechanics, 1971.

[14] Pian, T. H. H., "Element Stiffness Matrices for Boundary Compatibility and for Prescribed Boundary Stresses," *Proceedings of the First Conference of Matrix Methods in Structural Mechanics*, AFFDL-TR-66-80, 1967, Air Force Flight Dynamics Lab., Wright-Patterson Air Force Base, Ohio, pp. 457–477.

[15] Tong, P., "New Displacement Hybrid Finite Element Model for Solid Continua," *International Journal for Numerical Methods in Engineering*, Vol. 2, Jan. 1970, pp. 73–83.

[16] Atluri, S., "Static Analysis of Shells of Revolution Using Doubly-Curved Quadrilateral Elements Derived from Alternate Variation Models," SAMSO TR-69-284, Norton Air Force Base, Calif., 1969.

[17] Atluri, S. N., Kobayashi, A. S., and Nakagaki, M., "An Assumed Displacement Hybrid Finite Element Method for Fracture Mechanics," *International Journal of Fracture Mechanics*, Vol. 11, April 1975, pp. 257–271.

[18] Sih, G. C., Paris, P. C., and Erdogan, F., "Crack Tip Stress Intensity Factors for Place Extension and Plate Bending Problems," *ASME Transactions, Journal of Applied Mechanics*, Vol. 40, Ser. E, June 1962, pp. 306–312.

[19] Atluri, S., "A New Assumed Stress Hybrid Finite Element Model for Solid Continua," *AIAA Journal*, Vol. 9, Aug. 1971, pp. 1647–1649.

[20] Bowie, O. L. and Neal, P. M., "A Note on the Central Crack in a Uniformly Stressed Strip," *International Journal of Fracture Mechanics*, Vol. 2, Nov. 1970, pp. 181–182.

[21] Bowie, O. L., "Solutions of Plate Crack Problems by Mapping Technique," *Mechanics of Fracture I, Methods of Analysis and Solutions of Crack Problems*, edited by G. C. Sih, Noordhoff, Netherlands, 1973, pp. 1–55.

[22] Bowie, O. L. and Freese, C. E., "Central Cracks in Plane Orthotropic Plates," *International Journal of Fracture Mechanics*, Vol. 8, March 1972, pp. 49–58.

[23] Srawley, J. E. and Brown, W. F., "Fracture Toughness Testing," ASTM STP 381, 1965, pp. 133–196.